Journal of Solid State Chemistry **145,** 58–64 (1999)
Article ID jssc.1999.8219, available online at http://www.idealibrary.com on IDEAL®

Nonadiabatic Hopping Conduction in $Sr_{1+x}La_{1-x}FeO_4$ ($0 \leq x \leq 0.20$) below 300 K

N. Nakamura[1] and E. Iguchi

Materials Science, Department of Mechanical Engineering and Materials Science, Faculty of Engineering, Yokohama National University, Tokiwadai, Hodogaya-Ku, Yokohama, 240-8501 Japan

Received September 22, 1998; accepted February 3, 1999

We measured bulk conductivities using complex-plane impedance analyses and frequency dependencies of dielectric properties in $Sr_{1+x}La_{1-x}FeO_4$ ($0 \leq x \leq 0.20$) with the four-probe dc conductivities. The temperature dependence of bulk conductivity in every specimen exhibits the nonadiabatic hopping conduction; i.e., $\sigma = A_0 \exp[-(W_H + W_O/2)/k_BT]/T^{3/2}$, W_H and W_O being the hopping energy and the energy required to create a free hopping polaron. In every specimen, a dielectric relaxation process shows up with an activation energy nearly equal to that of the bulk conduction. The electron transfer integrals, J, estimated in the dielectric relaxations meet the nonadiabatic requirements; i.e., $J < 4W_H$ and $J < (4W_H k_B T)^{1/4}(\hbar\omega_{OL})^{1/2}$, where ω_{OL} is the frequency of the longitudinal optical mode. Speculation on the pre-exponential factor of the conductivity, A_0, indicates that the holes in valence bands created by electron excitation predominantly contribute to electrical transport rather than the doped holes introduced by Sr-substitution for La. The experimental results are explained self-consistently by nonadiabatic hopping conduction.

1. INTRODUCTION

Since the discovery of high-T_c oxides (1), physical properties and electronic structures of strongly correlated oxides of the K_2NiF_4 structure have been extensively studied. Hole-doped $Sr_{1+x}La_{1-x}FeO_4$ with the K_2NiF_4 structure has been also investigated using optical spectroscopies such as UPS and XAS, ^{57}Fe Mössbauer spectra, and magnetic properties (2–5). The end member $SrLaFeO_4$ is an intermediate-type oxide between Mott–Hubbard and charge-transfer insulators (4). ^{57}Fe Mössbauer measurements (3) indicate that a relatively large fraction of Fe ions is partially oxidized toward Fe^{4+} upon hole-doping. O K-edge and Fe K-edge X-ray-absorption measurements show that the whole valence band is constructed from well-mixed Fe 3d and O 2p states and that new hole bands composed of O 2p and Fe 3d states are formed in the original conduction-band edge upon hole-doping (upper Hubbard bands) (4). Omata *et al.* (5) carried out the optical absorption measurements in the range of 0.5–5 eV and dc conductivity measurements as a function of temperature, obtained the linear relation between the absorption intensity of the band maxima in the near infrared region ($\sim$1.2 eV) and the dc conductivities at room temperature, and argued that the newly formed unoccupied states were localized hole-states corresponding to the small polaron states and the near infrared band was due to the optically induced polarons hopping which resulted in the temperature dependence of the conductivity of $\sigma = A_0 \exp(-Q/k_BT)/T^{3/2}$, i.e., the nonadiabatic hopping conduction (6, 7).

It is, however, rather difficult to identify the type of small polarons, adiabatic or nonadiabatic, if only the temperature dependence of conductivity is used, because the conductivity subject to the adiabatic small polaron conduction also satisfies currently the temperature dependence of the nonadiabatic hopping conduction. Furthermore, a hopping process of nonadiabatic small polarons requires several restrictions on the electron transfer integral between neighboring hopping sites. These restrictions are then to be the criterion of judgment whether the hopping conduction is termed adiabatic or nonadiabatic (6–10).

After the discovery of high T_c superconductivity in the layer perovskite, $La_{2-x}Ba_xCuO_4$ (1), the investigation on polarons attracted markedly increased attention because polaronic conduction plays an important role in electrical transports in strongly correlated oxides like $Sr_{1+x}La_{1-x}FeO_4$. Although there are many ways of addressing polaron dynamics, the dielectric measurement can provide important information because a hopping process of small polarons has a high probability of involving a dielectric relaxation process (11–19) and, in the nonadiabatic case, the electron transfer integral is to be obtained from the dielectric measurements (6, 7). If nonadiabatic hopping conduction is realized in $Sr_{1+x}La_{1-x}FeO_4$, therefore, the dielectric

[1] Current address: Inorganic Materials and Polymers Laboratory, Fujitsu Laboratories, 10-1, Morinosato-Wakamiya, Atsugi, 243-0197 Japan.

0022-4596/99 $30.00

experiment is an indispensable means which provides significant knowledge on the polaronic conduction.

The present study employs polycrystalline ceramics specimens because single crystals of $Sr_{1+x}La_{1-x}FeO_4$ are difficult to produce. The single crystal approach is the most straightforward and the most common. Even if a polycrystalline ceramics sample is used, however, the complex-plane impedance analysis can distinguish bulk conduction from other types of conduction such as that across grain boundaries (19–23). Our previous reports indicate that the dc conductivities by the four-probe method include the grain-boundary effect which is somewhat serious in the investigation of the bulk conduction because grain boundaries in sintered oxides interfere with studying the transport phenomena (17, 19). If bulk conduction is available experimentally in the $Sr_{1+x}La_{1-x}FeO_4$ system, conduction behavior somewhat different from the result reported in the previous literature is expected.

Motivated by these factors, the elucidation of bulk conduction in $Sr_{1+x}La_{1-x}FeO_4$ ($0 \le x \le 0.2$) has been carried out by using the combination of the complex-plane impedance analysis and the dielectric measurement with the dc conductivity measurement by the four-probe method.

2. EXPERIMENTAL DETAILS

The specimens of $Sr_{1+x}La_{1-x}FeO_4$ ($0 \le x \le 0.2$) were prepared by the conventional solid-state reaction technique using La_2O_3, $SrCO_3$, and Fe_2O_3 powders (4N grades). The mixture was calcined in air at 1000°C for 24 h. After grinding, the calcined powder was pressed into pellets, finally sintered in air at 1400°C for 24 h, and then annealed at 700°C for 50 h in the pure flowing oxygen. The powder diffraction of every specimen using a Cu$K\alpha$ X-ray indicates a single phase of a tetragonal structure (14/*mmm*) with the lattice parameters nearly equal to those obtained previously (3, 24–26). The diffraction patterns are in very good agreement with that in JCPDS (Code 29-1305). The grain size of the specimens was found to be $\sim 1\,\mu m$ on average by scanning microscope studies. The densities of the specimens were 82–90% of the theoretical values.

Capacitance and impedance were measured as a function of temperature up to 300 K by the four-terminal pair ac impedance measurement method, using an HP 4284A LCR meter with a frequency range of 100 Hz to 1 MHz. The measured values of capacitance and impedance were corrected by calibrating capacitance and resistance of leads to zero. Flat surfaces of a specimen were coated with an In–Ga alloy in a 7 : 3 ratio by a rubbing technique for an electrode. Evaporated gold was also used for the electrode, but no significant difference was found in experimental results. A Maxwell–Wagner type polarization due to heterogeneity in a specimen is excluded because there are no significant differences in frequency dependencies of the dielectric constant at room temperature even if the thickness of the specimen of $x = 0.0$ is reduced from 1.1 to 0.5 mm.

A Keithley 619 resistance bridge, an Advantest TR 6871 digital multimeter, and an Advantest TR 6871 power supply were used for dc conductivity measurements by the four-probe method. The copper–constantan thermocouple precalibrated at 4.2, 77, and 273 K was used for temperature measurements.

3. EXPERIMENTAL RESULTS

Following the detailed account of the theoretical treatment (20–23), the complex-plane impedance analyses were carried out. Usually, in polycrystalline specimens, three independent semicircular arcs show up in the impedance plots where the real part (Z') of the total impedance is plotted against the imaginary part (Z'') as a parametric function of frequency, f, i.e., the highest-frequency arc corresponding to the bulk conduction, the intermediate-frequency arc due to the conduction across the grain boundary, and the lowest-frequency arc coming from the transport across the electrode–specimen interface. The resistance values of the circuit elements (bulk, grain boundary, and interface) are obtained from the real axis intercepts. Figure 1 depicts complex-plane impedance plots at 176, 236, and 296 K for the specimen of $x = 0.0$. The plots at 236 and 296 K contain a two semicircular-arcs structure, the highest- and intermediate-frequency arcs, while there is only the highest-frequency arc at 176 K. In $SrLaFeO_4$, for example, the plots of the highest-frequency arcs at temperatures higher than 300 K require frequencies much higher than the maximum one in the present work, i.e., 1 MHz. Since the lowest-frequency arc was not observed in any specimen at any temperature, there must be no polarization in the electrode–specimen interface. The highest resistance value of the intermediate-frequency arc is theoretically the total resistance in grains and boundaries.

Employing three sorts of conductivities, i.e., the bulk conductivity, the conductivity obtained from the highest resistance value of the intermediate-frequency arc, and the dc conductivity, Fig. 2 demonstrates three Arrhenius relations of $\sigma \cdot T^{3/2}$ and $1/T$ for the specimen of $x = 0.05$. The bulk conductivity is remarkably high but the plots of the other two Arrhenius relations overlap one another. Then the four-probe dc method measures the total resistance in grains and boundaries. Figure 3 displays the Arrhenius plots of $\sigma T^{3/2}$ and $1/T$ for all the specimens, where σ is the bulk conductivity. Every specimen contains a linear portion at higher temperatures, i.e., $\sigma = A_0 \exp(-Q/k_B T)/T^{3/2}$, where Q is the activation energy required for the bulk conduction, while the onset of non-Arrhenius bulk conduction at lower temperatures is found. In the linear portions, $Q = 0.43$, 0.30, 0.26, and 0.18 eV with $A_0 = 6.6 \times 10^7$, 3.9×10^6, 2.1×10^6, and $2.8 \times 10^5\ \Omega^{-1}\,cm^{-1}\,K^{3/2}$ for the

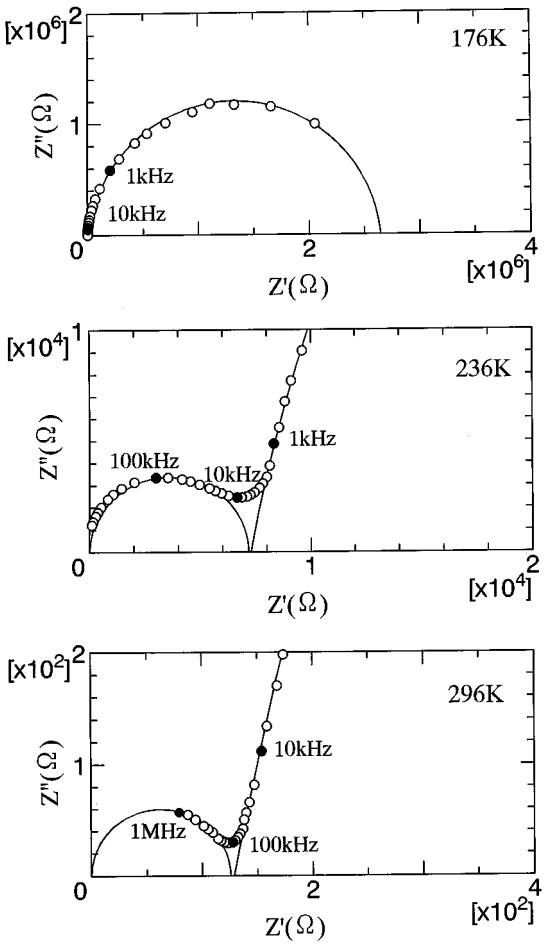

FIG. 1. Complex-plane impedance analyses for the specimen of $x = 0.0$ at 176, 236, and 296 K.

specimens of $x = 0.0$, 0.05, 0.1, and 0.2, respectively. The activation energies, Q, are somewhat different from the result of Omata *et al.*, i.e., 0.31, 0.20, 0.20, and 0.18 eV for $x = 0.0$, 0.1, 0.2, and 0.3 (5). If the bulk conduction is termed adiabatic, the Arrhenius plots of $\sigma \cdot T$ and $1/T$ yield slightly lower activation energies, but the general feature does not differ so much from Fig. 3.

A dielectric relaxation shows up in the loss factor (ε''), loss tangent ($\tan\delta$), impedance (imaginary part, Z''), and electric modulus (imaginary part, M'') of every specimen. In Fig. 4, the dielectric loss factor, ε'', of the specimen of $x = 0.05$ is plotted against the applied frequency at temperatures between 201 and 281 K at 8 K increments. The maximum of the dielectric loss factor at the resonance frequency f_ε, i.e., ε''_{max}, increases as the temperature is raised. This behavior suggests that the spectral intensity of the dielectric relaxation is thermally activated as well as dielectric relaxations occurring in other various materials in which hopping processes of small polarons dominate electrical transports (11–19).

4. DISCUSSION

Though the bulk conductivities and the dielectric relaxation processes observed in $Sr_{1+x}La_{1-x}FeO_4$ ($0 \le x \le 0.2$) seem surely to favor the polaronic scenario in the electrical transports, careful examinations are required. The present study includes several points to account for: (i) the type of majority carriers in $Sr_{1+x}La_{1-x}FeO_4$, nonadiabatic small polarons or adiabatic, (ii) the rather high conductivity of $SrLaFeO_4$ which is theoretically an insulator because $SrLaFeO_4$ is in a high-spin state, i.e., Fe^{3+} ($t_{2g\uparrow}^3 e_{g\uparrow}^2$) (27), and (iii) the number of carriers responsible for the bulk conduction.

4.1. Hopping Process of Small Polarons

Arrhenius relations in Fig. 3 imply that the bulk conduction in the $Sr_{1+x}La_{1-x}FeO_4$ system is termed nonadiabatic (6, 7). As described in the previous section, the peak due to the dielectric relaxation process shows up in the loss factor, loss tangent, impedance, and electric modulus. In Fig. 5, the normalized values of these dielectric properties are plotted

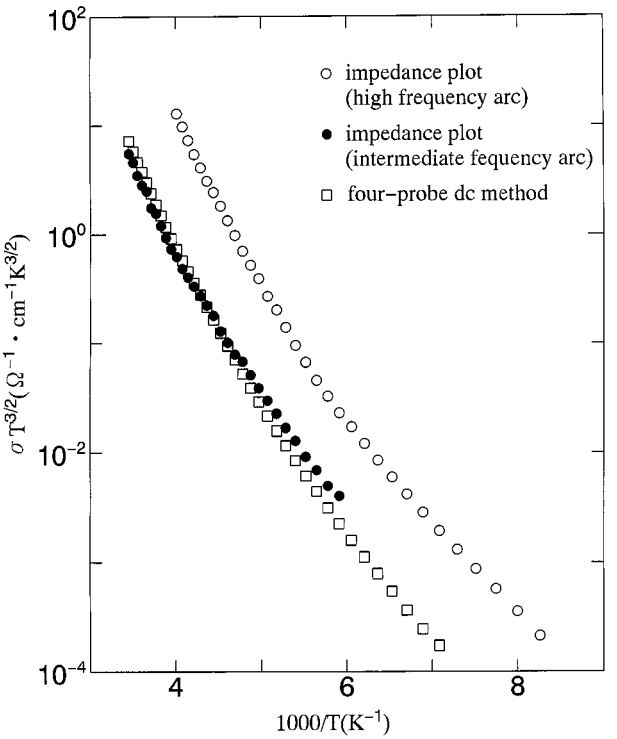

FIG. 2. Three Arrhenius relations of $\sigma \cdot T^{3/2}$ vs $1/T$ for the specimen of $x = 0.05$; the first one (open circles) represents the bulk conductivities obtained from the real axis intercepts of the highest-frequency arcs in the impedance analyses, the second one (solid circles) employs the highest resistances of the intermediate-semicircular arcs, and the third one (open squares) indicates the dc conductivities obtained by the four-probe method.

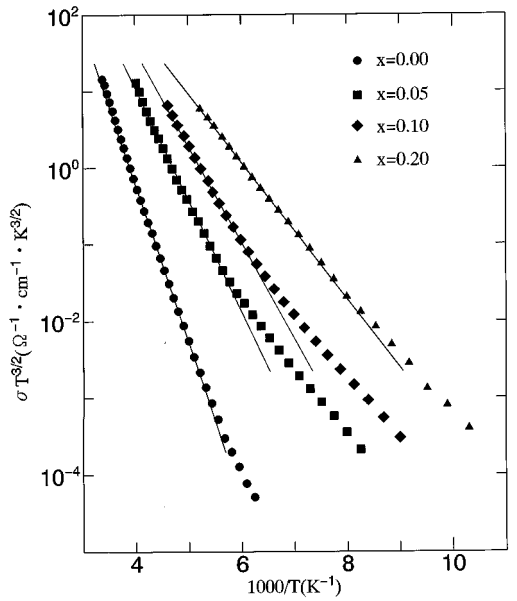

FIG. 3. Arrhenius plots of $\sigma \cdot T^{3/2}$ vs $1/T$ for the specimens of $x = 0.00$ (solid circles), 0.05 (solid squares), 0.10 (solid diamonds), and 0.20 (solid triangles), where σ is the bulk conductivity. The straight line represents the linear portion for every specimen.

against the applied frequency at $T = 185$ K for the specimen of $x = 0.10$. The peaks appear at different frequencies, though they come from the same relaxation process. Theoretically, the sequence of $f_\varepsilon < f_{\tan\delta} < f_Z \leq f_M$ holds when a dielectric relaxation process occurs within grains, where f_ε, $f_{\tan\delta}$, f_Z, and f_M are the resonance frequencies of the loss factor, loss tangent, impedance, and modulus (28). The result in Fig. 5 coincides with this theoretical prediction. This

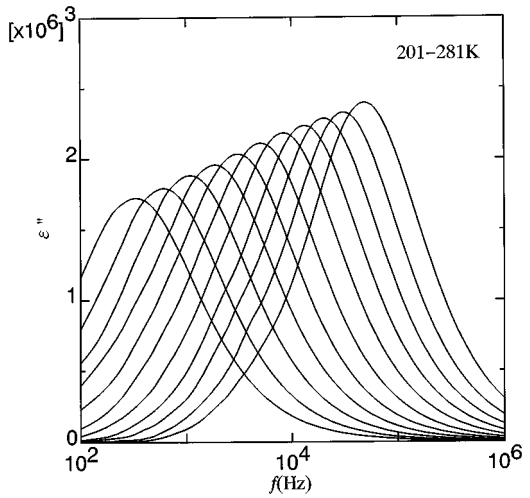

FIG. 4. Frequency dependencies of dielectric loss factor (ε'') as a parametric function of temperature of 201 to 281 K at 8 K increments for the specimen of $x = 0.05$.

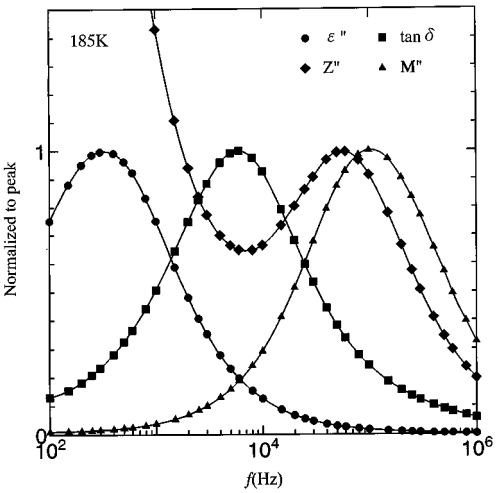

FIG. 5. The same relaxation process using the normalized dielectric loss factor (ε''), loss tangent ($\tan\delta$), imaginary part of impedance (Z''), and imaginary part of electric modulus (M'') at 185 K for the specimen of $x = 0.10$.

fact ensures that the dielectric relaxation process observed in Fig. 4 occurs within grains. In Fig. 5, there is another peak in the impedance at a very low frequency, which comes from the relaxation process in the grain boundaries causing the intermediate-frequency arc in Fig. 1.

The dielectric behavior in the present study is described approximately by Debye's theory (28, 29). At a temperature T, then, the resonance condition for the loss factor is $2\pi f_\varepsilon \tau = 1$, where $\tau = \tau_0 \exp(Q'/k_B T)$, Q' being the activation energy required for the dielectric relaxation process. Figure 6a demonstrates the Arrhenius relations of $f_\varepsilon T^{1/2}$ and $1/T$. This figure employs the realistic dielectric loss factor values which were obtained by subtracting the low-frequency contribution in a similar way to Lalevic *et al.* (30). The least-mean-square analyses yield $Q' = 0.40$, 0.28, 0.24, 0.16, and 0.15 eV for the specimens of $x = 0.0$, 0.05, 0.1, and 0.2, respectively.

The increase in the maximum of the loss factor with increasing temperature (see Fig. 4) is due to the thermal activation in the amount of the current carriers responsible for the dielectric relaxation process. This phenomenon is also explained by Debye's theory. In the nonadiabatic case, the maximum of the dielectric loss factor is given as $\varepsilon''_{\max} \propto \exp(-W_O/2k_B T)/T$, where W_O is the energy required to create a free hopping polaron. Figure 6b plots the Arrhenius relations between $\varepsilon''_{\max} \cdot T$ and $1/T$. Good straight lines are obtained with $W_O = 0.08$, 0.08, 0.05, and 0.05 eV for the specimens of $x = 0.0$, 0.05, 0.1, and 0.2, respectively.

The bulk conduction is represented by $\sigma = A_0 \exp(-Q/k_B T)/T^{3/2}$ as shown in Fig. 3. In the polaronic picture, the activation energies of the bulk conduction and the dielectric relaxation process are given as $Q \cong W_H + W_O/2$ and $Q' \cong W_H$, where W_H is the hopping energy of

polarons (8, 11–19, 31, 32). The disordered energy is omitted here because it is negligibly small compared with W_H in a crystalline lattice (33). In every specimen, the sum of the experimental values for W_H and $W_O/2$ is nearly equal to the activation energy required for the bulk conduction, Q, as expected theoretically. Namely the hopping process of small polarons is responsible for both the bulk conduction in Fig. 3 and the dielectric relaxation in Fig. 4. The hopping energy at $x = 0.0$ obtained here, 0.40 eV, is higher than the activation energy of Omata *et al.*, 0.31 eV (5), but 0.15 eV at $x = 0.2$ is conversely less than their result, 0.20 eV. This means that the hopping energy of the bulk conduction obtained here decreases rather rapidly as x increases.

4.2. Nonadiabatic Small Polarons

In the resonance condition of $2\pi f_\varepsilon \tau_0 \exp(Q'/k_BT) = 1$ for the loss factor, τ_0 in the nonadiabatic case is $2\hbar(W_H k_B T)^{1/2}/\pi^{1/2}J^2$, where J is the electron transfer integral between neighboring hopping sites, $\hbar$ is Plank's constant divided by 2π, and k_B is Boltzmann's constant (6, 7). Then the nonadiabatic resonance condition for the dielectric loss factor has the form of $f_\varepsilon T^{1/2} = J^2 \exp(-Q'/k_BT)/4\hbar(\pi W_H k_B)^{1/2}$. Using the experimental value for W_H, the extrapolations of the Arrhenius relations of $f_\varepsilon T^{1/2}$ and $1/T$ at $T \to \infty$ in Fig. 6a yield $J = 9.5 \times 10^{-3}$, 2.8×10^{-3}, 1.4×10^{-3}, and 0.30×10^{-3} eV for the specimens of $x = 0.0$, 0.05, 0.1, and 0.2.

According to Holstein and Emin (6, 7), the nonadiabatic case requires the following two restrictions for the electron transfer integral between hopping sites, i.e., $J < 4W_H$ and $J < (W_H k_B T)^{1/4}(\hbar\omega_{OL})^{1/2}$, where ω_{OL} is the frequency of the longitudinal optical mode. The frequency values of ω_{OL} in the $Sr_{1+x}La_{1-x}FeO_4$ system are not yet available but the experimental values in similar perovskite materials lie in the range 10^{13}–$10^{14}\ s^{-1}$ (34, 35). The first condition holds in every specimen because $J < W_H$. As for the second condition, the experimental values for W_H, the lowest temperatures in Arrhenius relations of Fig. 6a and $\omega_{OL} \cong 10^{13}\ s^{-1}$ yield $(W_H k_B T)^{1/4}(\hbar\omega_{OL})^{1/2} \cong 1.1 \times 10^{-2} \sim 1.9 \times 10^{-2}$ eV, larger than the experimental J values, $9.5 \times 10^{-3} \sim 0.3 \times 10^{-3}$ eV. Then, the second condition also holds for every specimen. An assessment like this meets definitely the requirements for nonadiabatic hopping conditions. Then the results in Figs. 3 and 6 are explained self-consistently in terms of the nonadiabatic hopping condition. Consequently the major carrier responsible for the bulk conduction in $Sr_{1+x}La_{1-x}FeO_4$ ($0 \le x \le 0.2$) is a nonadiabatic small polaron.

The optical results indicate the hole character of well mixed O $2p$ and Fe $3d$ states, i.e., a ligand hole (4). Then, overlapping of extended O $2p$ wave functions of holes is enhanced with increasing the amount of holes, which must lead to decreases in the hopping energy and the electron transfer integral.

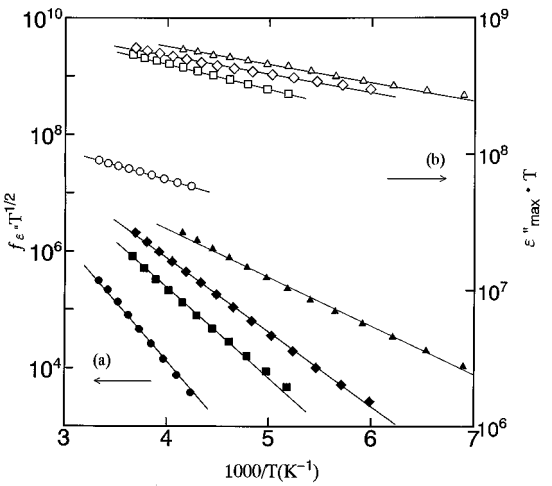

FIG. 6. (a) Arrhenius relations between $f_\varepsilon \cdot T^{1/2}$ and $1/T$ for the specimens of $x = 0.00$ (solid circles), 0.05 (solid squares), 0.10 (solid diamonds), and 0.20 (solid triangles), and (b) Arrhenius relations between $\varepsilon''_{max} \cdot T$ and $1/T$ for the specimens of $x = 0.00$ (open circles), 0.05 (open squares), 0.10 (open diamonds), and 0.20 (open triangles).

4.3. Density of Nonadiabatic Small Polarons Responsible for Bulk Conduction

As described before, Arrhenius plots of $\sigma = A_0 \exp[-(W_H + W_O/2)/k_BT]/T^{3/2}$ in Fig. 3 are justified. Despite the increase in the amount of Sr ions which create holes, however, the pre-exponential factor, A_0, decreases from 6.6×10^7 ($x = 0.0$) to $2.8 \times 10^5\ \Omega^{-1}\,cm^{-1}K^{3/2}$ ($x = 0.2$). If the hopping conduction is termed adiabatic, A_0 is directly proportional to the amount of hopping carriers (8, 31, 32). This is inconsistent with the present result. This fact rationalizes the nonadiabatic scenario again. In the nonadiabatic theory, $A_0 = zn_0e^2a^2\pi^{1/2}J^2/k_B^{3/2}\hbar W_H^{1/2}$, where z is the configuration number, a is the hopping distance and n_0 is the number of carriers localized at trapping sites at very low temperatures (36).

$SrLaFeO_4$ is originally an insulator but has a rather high conductivity. Furthermore the amount of nonadiabatic small polarons of holes increases by thermal excitation (see Fig. 6b). If this increase is ascribed only to the dissociation of the doped holes from the trapping sites, the transport property in the specimen of $x = 0.0$ is difficult to speculate because of no doped holes in $SrLaFeO_4$, i.e., $n_0 = 0$. If holes are created by thermal excitation of electrons in valence bands to upper levels separated from the top edge of the valence bands by $W_O = 0.08$ eV, n_0 is to be the number of electrons in the valence bands. $SrLaFeO_4$ is in a high-spin state, i.e., Fe^{3+} ($t_{2g\uparrow}^3 e_{g\uparrow}^2$) (27). When the thermal excitation of electrons in the $3d$ top bands of Fe^{3+}, i.e., $e_{g\uparrow}$-bands, is

predominant, $A_0 \cong 2 \times 10^7\ \Omega^{-1}\,cm^{-1}\,K^{3/2}$, while about $6 \times 10^7\ \Omega^{-1}\,cm^{-1}\,K^{3/2}$ when the electrons in O $2p$ bands, i.e., $(2p)^6$, are mainly responsible for this excitation, where the experimental values for W_H and J are employed in these assessments. The estimated values are very competitive with the experimental result, i.e., $A_0 = 6.6 \times 10^7\ \Omega^{-1}\,cm^{-1}\,K^{3/2}$.

In the case of $x = 0.05$, holes are created by Sr-substitution for La. These holes must be localized at trapping sites such as impurities at very low temperatures. Upon hole doping, a relatively large fraction of Fe ions is partially oxidized toward Fe^{4+} (3). In light hole doping, then, the most plausible trapping site must be the Fe site adjacent to Sr^{2+} ion, i.e., the Fe^{4+}–Sr^{2+} pair. If the doped holes govern the bulk conduction, $A_0 \cong 8 \times 10^3$–$2 \times 10^4\ \Omega^{-1}\,cm^{-1}\,K^{3/2}$, less than the experimental value by two or three orders. If the holes created by electron excitation from valence bands also govern the conduction, $A_0 \cong 2 \times 10^6$–$6 \times 10^6\ \Omega^{-1}\,cm^{-1}\,K^{3/2}$, which is close in values to the experimental result, $3.9 \times 10^6\ \Omega^{-1}\,cm^{-1}\,K^{3/2}$. The contribution due to the doped holes is very small in comparison with the holes created by electron excitation. A similar interpretation is possible for other specimens. It should be emphasized that a rapid decrease in the electron transfer integral, J, results in the decrease in the pre-exponential factor, A_0, with increasing x. The experimental relationship between A_0 and x is impossible to account for if based upon the adiabatic scheme. Omata *et al.* (5) obtained the values of the same order as ours for W_O. The extrapolation of their conductivity results (5) yields also the magnitudes in the same order as ours for A_0.

At lower temperatures, as shown in Fig. 3, non-Arrhenius conduction is found. Omata *et al.* (5) insist there is a linear Arrhenius relation between $\sigma \cdot T$ and $1/T$ at such low temperatures, which means that the carrier-type transfers from a nonadiabatic small polaron at higher temperatures to an adiabatic one at lower temperatures. To our knowledge, however, there is no literature which observed such a transition with decreasing temperature. Emin (37, 38) argues that the onset of a non-Arrhenius temperature dependence as temperature is lowered is the general feature of small polaron hopping. It arises as multiphonon jump processes are frozen out. Then, the onset of the non-Arrhenius bulk conduction observed at lower temperatures must be close to the picture constructed by Emin.

5. CONCLUSION

Using complex-plane impedance analyses, bulk conductivities in $Sr_{1+x}La_{1-x}FeO_4$ $(0 \le x \le 0.20)$ have been obtained and their temperature dependencies exhibit the nonadiabatic hopping conduction, i.e., $\sigma = A_0 \exp[-(W_H + W_O/2)/k_BT]/T^{3/2}$, where W_H and W_O are the hopping energy of nonadiabatic small polarons and the energy required for the thermally activated increase in the amount of current carriers. Every specimen contains a dielectric relaxation process with an activation energy nearly equal to that of the bulk conduction. The electron transfer integrals, J, estimated in the dielectric relaxation processes meet the nonadiabatic requirements, i.e., $J < 4W_H$ and $J < (4W_H k_B T)^{1/4}(\hbar\omega_{OL})^{1/2}$, where ω_{OL} is the frequency of the longitudinal optical mode. With increasing the amount of Sr, the magnitudes for A_0, W_H, W_O, and J decrease.

These experiments ensure that the majority carriers in $Sr_{1+x}La_{1-x}FeO_4$ $(0 \le x \le 0.20)$ are nonadiabatic small polarons of holes. In the speculation on the pre-exponential factor of the bulk conductivity A_0, the doped holes created by Sr-substitution for La alone cannot explain the experimental results and instead the holes in valence bands created by electron excitation to the upper levels predominantly contribute to the electrical transports. The upper levels are separated from the top edge of the valence bands by 0.08–0.05 eV. The decrease in A_0 with increasing x is mainly ascribed to the decrease in J. At lower temperatures, non-Arrhenius conduction is found in every specimen, which must be because multiphonons jump processes are frozen out.

ACKNOWLEDGMENTS

The authors are very grateful to W. H. Jung, N. Nakatsugawa, and Y. Nonaka for useful discussions and advice in this project. This project was supported by a Grant-in-Aid for Science Research (No. 08650812) from the Ministry of Education, Science and Culture, Japan, and Takahashi Industrial and Economic Research Foundation.

REFERENCES

1. J. G. Bednortz and K. A. Müller, *Z. Phys. B* **64,** 189 (1986).
2. T. Omata, K. Ueda, N. Ueda, M. Katada, S. Fujitsu, T. Hashimoto, and H. Kawazoe, *Solid State Commun.* **88,** 807 (1993).
3. T. Omata, K. Ueda, H. Hosono, M. Katada, N. Ueda, and H. Kawazoe, *Phys. Rev. B* **49,** 10194 (1994).
4. T. Omata, K. Ueda, H. Hosono, T. Miyazaki, S. Hasegawa, N. Ueda, and H. Kawazoe, *Phys. Rev. B* **49,** 10200 (1994).
5. T. Omata, H. Ikawa, S. Fujitsu, N. Ueda, H. Hosono, and H. Kawazoe, *Solid State Commun.* **97,** 411 (1996).
6. T. Holstein, *Annals Pys.* **8,** 343 (1959).
7. D. Emin, *Phys. Rev. B* **4,** 3639 (1971).
8. I. G. Austin and N. F. Mott, *Adv. Phys.* **18,** 41 (1969).
9. M. A. Kolber and R. K. MacCrone, *Phys. Rev. Lett.* **29,** 1457 (1972).
10. F. G. Koffyberg and F. A. Benko, *J. Non-Cryst. Solids* **40,** 7 (1980).
11. E. Iguchi, N. Kubota, T. Nakamori, N. Yamamoto, and K. J. Lee, *Phys. Rev. B* **43,** 8646 (1991).
12. E. Iguchi and K. Akashi, *J. Phys. Soc. Jpn.* **61,** 3385 (1992).
13. K. J. Lee, A. Iguchi, and E. Iguchi, *J. Phys. Chem. Solids* **54,** 975 (1993).
14. E. Iguchi and W. H. Jung, *J. Phys. Soc. Jpn.* **63,** 3078 (1994).
15. W. H. Jung and E. Iguchi, *J. Phys.: Condens. Matter* **7,** 1215 (1994).
16. E. Iguchi, T. Hashimoto, and S. Yokoyama, *J. Phys. Soc. Jpn.* **65,** 221 (1996).
17. E. Iguchi, K. Ueda, and W. H. Jung, *Phys. Rev. B* **54,** 17431 (1996).
18. W. H. Jung and E. Iguchi, *Philos. Mag. B* **73,** 873 (1996).

19. E. Iguchi, N. Nakamura, and A. Aoki, *J. Phys. Chem. Solids* **58,** 755 (1997).
20. J. E. Bauerle, *J. Phys. Chem. Solids* **30,** 2657 (1969).
21. J. R. MacDonald, *J. Chem. Phys.* **61,** 3977 (1974).
22. A. D. Franklin, *J. Amer. Ceram. Soc.* **58,** 465 (1975).
23. J. R. MacDonald, *in* "Superionic Conductors," p. 1. Plenum, New York, 1976.
24. L. Soubeyroux, P. Courbin, L. Forunes, D. Fruchart, and G. leFlem, *J. Solid State Chem.* **31,** 313 (1980).
25. Y. Takeda, K. Imayoshi, N. Imayoshi, O. Yamamoto, and M. Takano, *J. Mater. Chem.* **4,** 19 (1994).
26. S. Fujihara, T. Nakata, H. Kawazoe, and T. Yoko, *J. Solid State Chem.* **115,** 456 (1995).
27. K. K. Singh, P. Ganguly, P. P. Edwards, and J. B. Goodenough, *J. Phys.: Condes. Matter* **3,** 2479 (1991).
28. R. Gerhardt, *J. Phys. Chem. Solids* **55,** 1491 (1994).
29. H. Frölich, *in* "Theory of Dielectrics," p. 70. Clarendon, Oxford, 1958.
30. B. Lalevic, N. Fuschillo, B. Kuliyev, and W. Wang, *Appl. Phys.* **5,** 127 (1974).
31. I. G. Lang and Yu. A. Firsov, *Soviet Phys. JETP* **54,** 826 (1968).
32. D. Emin and T. Holstein, *Annals Phys.* **53,** 439 (1969).
33. L. A. K. Dominik and R. K. MacCrone, *Phys. Rev.* **163,** 756 (1967).
34. J. C. Phillips, *in* "Physics of High-T_c Superconductors," Chap. 4. Academic Press, San Diego, 1989.
35. R. Raffaelle, H. U. Anderson, C. D. Sparlin, and P. E. Parris, *Phys. Rev. B* **43,** 7991 (1991).
36. L. Murawski, C. H. Chung, and J. D. Mackenzie, *J. Non-Cryst. Solids* **32,** 91 (1979).
37. D. Emin, *Phys. Rev. Lett.* **32,** 303 (1974).
38. D. Emin, *Adv. Phys.* **24,** 305 (1982).